

interpretation of our earlier experiments reported in a previous paper⁴ must be discarded.

Further experiments are planned at lower temperatures in the presence of electric fields to explore the He II scintillation process further. With the more detailed information which these and other experiments should provide, an understanding of the temperature dependence exhibited in Figs. 2-4 may be achieved.

ACKNOWLEDGMENTS

We wish to thank Professor Kerson Huang of the Massachusetts Institute of Technology for helpful comments relating to ion-vortex ring interactions. We wish, also, to acknowledge the contributions of Dr. Frank E. Moss in connection with the design of the rotating vacuum seal and other equipment which was used.

Lambda Transformation of Liquid He⁴ at High Pressures*

HENRY A. KIERSTEAD

Argonne National Laboratory, Argonne, Illinois

(Received 10 August 1966)

Measurements are reported of the pressure coefficient $\beta_V = (\partial P/\partial T)_V$ of He⁴ I and He⁴ II along the isochore which crosses the λ line at $T_\lambda = 1.7683^\circ\text{K}$ and $P_\lambda = 29.56$ atm, and of the compressibility $\rho\kappa_T = (\partial\rho/\partial P)_T$ along the isotherm $T = 1.7683^\circ\text{K}$, the closest points being 2.5 μdeg , 50 μatm , and 10^{-7} g/cm^3 from the lambda line in temperature, pressure, and density, respectively. The data are well represented by the equations:

$$\text{He II: } \beta_V = -14.22 + 3.54 \log_{10}(T_\lambda - T), \quad 2.4 \times 10^{-6} \leq T_\lambda - T \leq 3 \times 10^{-3}$$

$$\text{He I: } \beta_V = 9.00 + 7.50 \log_{10}(T - T_\lambda), \quad 2.5 \times 10^{-6} \leq T - T_\lambda \leq 6 \times 10^{-3}$$

$$\text{He II: } (\rho\kappa_T)^{-1} = 1000.4 + 78.9 \log_{10}(\rho_\lambda - \rho), \quad 10^{-7} \leq \rho_\lambda - \rho \leq 10^{-5}$$

$$\text{He I: } (\rho\kappa_T)^{-1} = 1675.0 + 167.2 \log_{10}(\rho - \rho_\lambda), \quad 10^{-7} \leq \rho - \rho_\lambda \leq 10^{-5},$$

where T is in $^\circ\text{K}$, ρ in g/cm^3 , β_V in $\text{atm}/^\circ\text{K}$, and $\rho\kappa_T$ in $\text{g cm}^{-3}/\text{atm}$. Although these measurements have been extended by a factor of 10 closer to the λ line than ever before, they continue to agree with a logarithmic form which cannot be correct at the λ line.

INTRODUCTION

THE thermodynamic properties of liquid He⁴ change very rapidly close to the lambda transformation. Consequently, in order to investigate the nature of the transformation, it is necessary to make measurements extremely close to the lambda line. Since the anomalous behavior is spread out over a larger temperature interval at high pressures, it is most advantageous to work near the upper lambda point (T_λ, P_λ), where the lambda curve meets the melting curve.

Our earlier measurements¹ of the pressure coefficient, $\beta_V = (\partial P/\partial T)_V$, were made along that isochore which passes through the upper lambda point, and, therefore, could be made only in He I (above the lambda temperature), since the isochore is in the solid region of the phase diagram below the lambda temperature. In this paper, we present measurements of the pressure coefficient and of the compressibility, $\rho\kappa_T = (\partial\rho/\partial P)_T$, of both He I and He II near the point $T_\lambda = 1.7683^\circ\text{K}$, $P_\lambda = 29.56$ atm, which is on the lambda curve 5.0 mdeg above the upper lambda point. The closest points were 2.5 μdeg , 50 μatm , and 10^{-7} g/cm^3 from the lambda line in tem-

perature, pressure, and density, respectively. Thus, our measurements of the pressure coefficient and of the compressibility were an order of magnitude closer to the lambda point than were those of Lounasmaa,² whose measurements, in turn, were two orders of magnitude closer than the best previous measurements.^{3,4} The resolution of the apparatus was about 0.5 μdeg in temperature, 1 μatm in pressure, and 10^{-9} g/cm^3 in density ($\Delta\rho/\rho = 5 \times 10^{-9}$).

EXPERIMENTAL

The apparatus used in these experiments is similar to that used previously.^{1,5} It is shown schematically in Fig. 1.

Helium gas was purified in a trap (not shown) immersed in liquid helium and was condensed into the sample compartment G through the low-temperature valve A, which was kept closed during measurements. G was isolated from the liquid-helium bath by the vacuum case B. Its temperature was controlled by the heater F and by pumping on liquid helium in E.

² O. V. Lounasmaa, *Phys. Rev.* **130**, 847 (1963)

³ O. V. Lounasmaa and L. Kaunisto, *Ann. Acad. Sci. Fennicae: Ser. A VI*, **59** (1960).

⁴ E. R. Grilly and R. L. Mills, *Ann. Phys. (N. Y.)* **18**, 250 (1962).

⁵ H. A. Kierstead, *Phys. Rev.* **144**, 166 (1966).

* Based on work performed under the auspices of the U. S. Atomic Energy Commission.

¹ H. A. Kierstead, *Phys. Rev.* **138**, A1594 (1965).

The absolute pressure of the sample was read to 0.01 atm on the stainless-steel Bourdon gauge⁶ P, which was calibrated against a dead-weight tester. Pressure changes were measured by means of the differential quartz helix Bourdon gauge⁷ K with a stainless-steel high-pressure reference capsule L. The reference pressure was maintained constant by connecting the reference capsule to a large reservoir Q of helium gas in a well-stirred ice bath. The quartz Bourdon tube and reference capsule were filled with Apiezon B oil,⁸ and the stainless steel Bourdon tube was filled with mercury, in order to reduce the dead space. It was necessary to correct for changes in temperature of the small volumes of gas in the dead space at room temperature and at the Bourdon-gauge temperature. A correction was also made for thermal expansion of the oil in the Bourdon gauge. The gauge was sensitive to pressure changes of 10^{-6} atm, but the precision of the pressure measurements was limited to two or three times 10^{-5} atm by uncertainty of the dead-space corrections to the reference pressure.

The proper sample density was obtained by filling through the low-temperature valve to such a pressure that the lambda transition occurred at 5.0 mdeg above the upper lambda temperature. The low-temperature valve was then closed. For compressibility measurements, the density was varied by changing the position of the stem of needle valve J, thus forcing helium from the dead space of the valve into the sample cell G, or

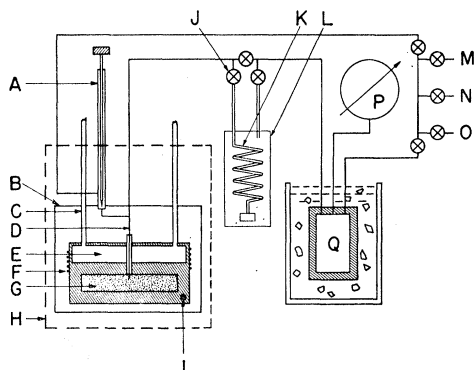


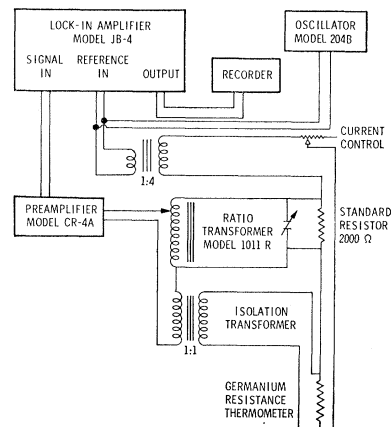
FIG. 1. Schematic drawing of the apparatus. (A) needle valve; (B) vacuum case; (C) pumping and vapor pressure tubes (2) for (E); (D) 30% Cu-Ni capillary tubing, 0.1 mm i.d.; (E) temperature and vapor pressure compartment; (F) heater; (G) sample compartment packed with fine copper wire for rapid equilibrium (volume 39.83 cm^3 at 1.76°K , height 10 mm to keep hydrostatic pressure differences small); (H) dashed lines enclose space immersed in liquid-helium bath; (I) germanium thermometer; (J) needle valve used as density control; (K) quartz bourdon tube with resolution of 10^{-6} atm; (L) reference capsule; (M) to He^4 supply tank and purifier; (N) to pump; (O) to atmosphere; (P) 35-cm dial test gauge calibrated against a dead-weight tester; (Q) ballast volume (1461 cm^3) for balancing the right-hand side of K, held at constant temperature by an ice bath; \otimes needle valves.

⁶ Heise Bourdon Tube Company, 35-cm dial, 1000 psi, graduated at 1 psi intervals.

⁷ Texas Instruments, Inc., Model 140, capsule type 4, bourdon tube No. 14 (0–75 mm).

⁸ Apiezon Products, Ltd.

FIG. 2. ac potentiometer circuit for germanium resistance thermometer.



vice versa. The valve had a $\frac{1}{8}$ -in.-diam stem and was threaded with 56 threads per inch. Therefore, one revolution of the stem displaced a volume of $3.67 \times 10^{-3} \text{ cm}^3$ of helium gas, which changed the sample density by $4.45 \times 10^{-7} \text{ g/cm}^3$. The valve was provided with a pointer and a dial plate calibrated in degrees so that the rotation of the stem could be measured to one degree, providing a resolution of about 10^{-9} g/cm^3 in density.

Temperatures were measured with germanium resistance thermometers in an ac potentiometer circuit, using a 7-dial Gertsch Model 1011R ratio transformer as the balancing element and a Princeton Applied Research Corporation Model CR-4A Low-Noise Amplifier and Model JB-4 Lock-in Amplifier as null detector. The measuring current was obtained from a Hewlett-Packard Model 204B audio oscillator. The frequency was about 300 cps. The measuring circuit is shown in Fig. 2. Three different germanium resistance thermometers were used: a Honeywell Series IV with a resistance at 1.76°K of 1210Ω and a sensitivity of $855 \mu\text{deg}/\Omega$, a Cryocal with a resistance of 2140Ω and a sensitivity of $350 \mu\text{deg}/\Omega$, and a Radiation Research Series CG-1 with a resistance of 1844Ω and a sensitivity of $405 \mu\text{deg}/\Omega$. With about $14 \mu\text{A}$ of measuring current, the resistance could be measured with a precision of one-half part per million. The $2000\text{-}\Omega$ standard resistor had a temperature coefficient of two parts per million per $^\circ\text{C}$ and was mounted in an insulated aluminum block with a thermal time constant of over 6 h.

The resistance thermometers were calibrated against the vapor pressure of helium in E on the T_{58} scale,⁹ using a tube separate from the pumping tube. We believe that our temperature scale agrees with the T_{58} scale to better than $10^{-4} \text{ }^\circ\text{K}$ in absolute temperature, and to one part per thousand for temperature differences.

For measurements of the pressure coefficient, the density was held constant, except for small changes caused by variation of the temperature and pressure

⁹ H. Van Dijk, M. Durieux, J. R. Clement, and J. K. Logan, Natl. Bur. Std. (U. S.), Monograph 10 (1960).

of the gas in the dead space. This effect was corrected for as explained below.

The lambda point was observed before each set of measurements, in the following way. With the sample below the lambda temperature, the heater current was adjusted so that the sample temperature increased at a rate of about 10^{-5} deg/min, at constant density, and the temperature was plotted on a strip-chart recorder. Because of the abrupt change in thermal conductivity at the lambda transformation, the heating curve showed a sharp break, which could be located to within a microdegree. The sample was then held at the lambda temperature until pressure equilibrium was established, and the lambda-point pressure was recorded.

The pressure coefficient β_V was measured by observing the pressure at a series of temperatures, at constant volume, starting at the lambda point. At each point the temperature was held constant until equilibrium was established.

The measured pressure coefficients were corrected to constant volume (constant density) by means of the thermodynamic relation

$$(\partial P/\partial T)_X = (\partial P/\partial T)_V + (\partial P/\partial \rho)_T (\partial \rho/\partial T)_X, \quad (1)$$

where X denotes the experimental path, which was not exactly at constant density. Rearranging (1) and using the definitions

$$\beta_V = (\partial P/\partial T)_V, \quad \rho\kappa_T = (\partial \rho/\partial P)_T, \quad (2)$$

we have

$$\beta_V = (\partial P/\partial T)_X - (\partial \rho/\partial T)_X / (\rho\kappa_T). \quad (3)$$

Our measurements were used for κ_T , and $(\partial \rho/\partial T)_X$ could be calculated from the temperatures and volumes of the dead spaces.

The compressibility was measured by determining the lambda point, then keeping the temperature constant while observing the pressure at a series of different densities, obtained by adjusting valve J.

RESULTS

The results of 258 measurements of the pressure coefficient are plotted against $T - T_\lambda$ in Fig. 3, and against $\log_{10}|T - T_\lambda|$ in Fig. 4. $T - T_\lambda$ is the distance from the lambda line, measured along an isochore. T_λ was in all cases within a few tenths of a millidegree of 1.7683°K. Measurements at nearly the same temperature, from different runs, were averaged. Data taken with the three different resistance thermometers and with two different Bourdon tubes agreed well with each other. The solid circles in Fig. 4 are taken from our previous measurements¹ near the upper lambda point. They are in good agreement with the present measurements even though the temperature was 5 mdeg lower.

The straight lines in Fig. 4 and the curves in Fig. 3

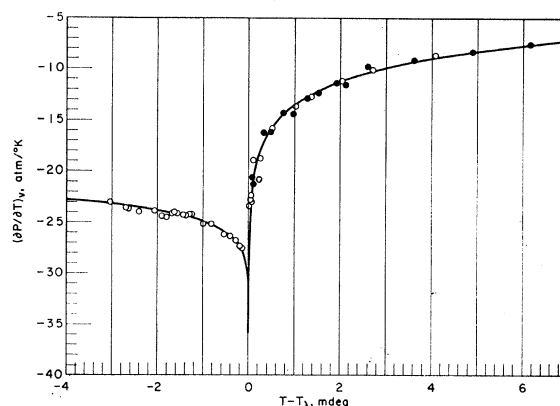


FIG. 3. Pressure coefficient of He⁴ along the isochore which crosses the lambda line at 1.7683°K. Points near T_λ are omitted for clarity. Open circles represent present measurements, closed circles represent those of Kierstead (Ref. 1).

are calculated from the equations

$$\beta_V = -14.22 + 3.54 \log_{10}(T_\lambda - T) \text{ atm/}^\circ\text{K} \quad (\text{He II}) \quad (4)$$

$$= 9.00 + 7.50 \log_{10}(T - T_\lambda) \text{ atm/}^\circ\text{K}. \quad (\text{He I}) \quad (5)$$

The form of these equations is the same as that used previously by us¹ and by Lounasmaa.^{2,3} Our data show a phenomenon that can be seen also in Lounasmaa's measurements² at 13 atm, namely, that β_V is more negative in He II than in He I, but varies more rapidly with $|T - T_\lambda|$ in He I. In fact, in our case the two lines cross at $|T - T_\lambda| = 1.37 \times 10^{-6}$ °K. Lounasmaa's lines (extrapolated) cross at 2×10^{-9} °K.

The results of 98 measurements of $(\partial \rho/\partial P)_T = \rho\kappa_T$ along the isotherm $T = 1.7683^\circ\text{K}$ are shown plotted against $P - P_\lambda$ in Fig. 5. $(\rho\kappa_T)^{-1}$ is plotted against $\log_{10}|\rho - \rho_\lambda|$ in Figs. 6 and 7. These data cover roughly the same range, in terms of distance from the lambda line, as the lower two decades of Fig. 4. The solid lines

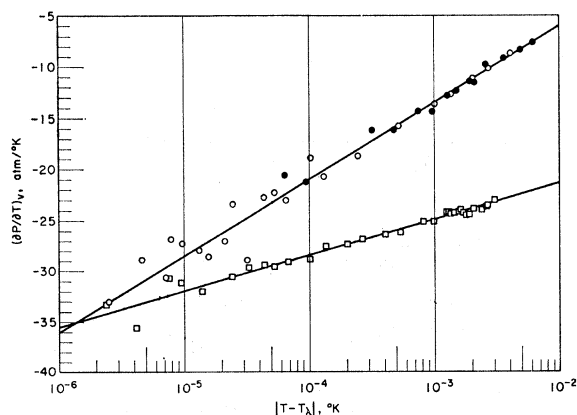


FIG. 4. Pressure coefficient of He⁴ along the isochore which crosses the lambda line at 1.7683°K; semilogarithmic plot; open circles represent He I; squares represent He II; closed circles represent the data of Kierstead (Ref. 1) for He I. Equations of lines: $\beta_V = 9.00 + 7.50 \log_{10}(T - T_\lambda)$ (He I); $\beta_V = -14.22 + 3.54 \log_{10}(T_\lambda - T)$ (He II).

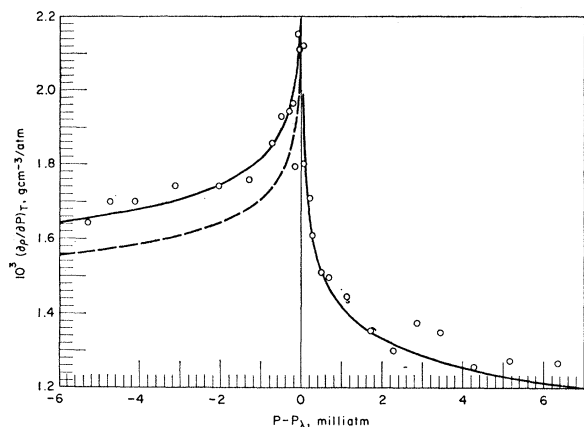


FIG. 5. $(\partial\rho/\partial P)_T$ of He⁴ along the isotherm $T=1.7683^\circ\text{K}$, against $P-P_\lambda$. Solid curves: Eqs. (6), (7), (8), and (9); dashed curve: Eqs. (23) and (25).

represent the equations

$$(\rho\kappa_T)^{-1} = 1000.4 + 78.9 \log_{10}(\rho_\lambda - \rho) \text{ atm cm}^3/\text{g} \quad (\text{He II}) \quad (6)$$

$$= 1675.0 + 167.2 \log_{10}(\rho - \rho_\lambda) \text{ atm cm}^3/\text{g} \quad (\text{He I}), \quad (7)$$

$$P - P(\rho_\lambda) = (\rho - \rho_\lambda)[966.1 + 78.9 \log_{10}(\rho_\lambda - \rho)] \text{ atm} \quad (\text{He II}) \quad (8)$$

$$= (\rho - \rho_\lambda)[1602.4 + 167.2 \log_{10}(\rho - \rho_\lambda)] \text{ atm} \quad (\text{He I}). \quad (9)$$

Equations (8) and (9) are the integrated forms of (6) and (7), respectively.

Figure 5 shows a much different pressure dependence than Lounasmaa's² Fig. 3, which indicated a linear dependence of κ_T on pressure, with a small discontinuity at the lambda point. Lounasmaa's failure to find a sharp rise in κ_T near the lambda point is due partly to the fact that the anomalous behavior is confined to a smaller pressure interval at lower pressures, and partly

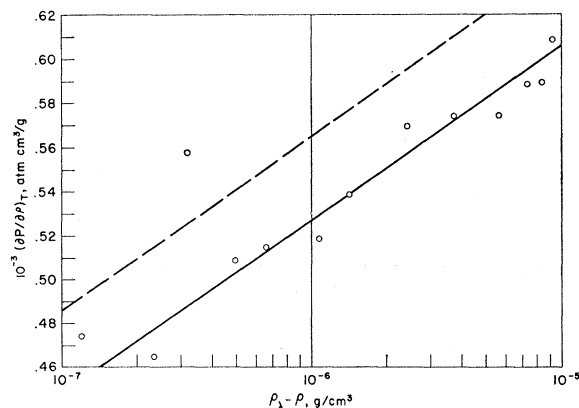


FIG. 6. $(\partial P/\partial\rho)_T$ of He⁴II along the isotherm $T=1.7683^\circ\text{K}$, against $\rho_\lambda - \rho$, semilogarithmic plot. Solid line: $(\rho\kappa_T)^{-1} = 1000.4 + 78.9 \log_{10}(\rho_\lambda - \rho)$; dashed line: $(\rho\kappa_T)^{-1} = 1038.2 + 78.9 \log_{10}(\rho_\lambda - \rho)$.

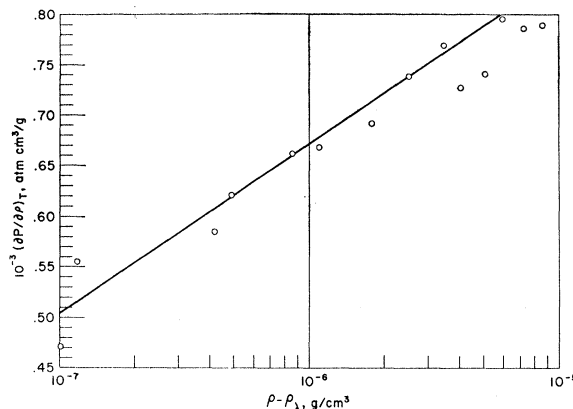


FIG. 7. $(\partial P/\partial\rho)_T$ of He⁴I along the isotherm $T=1.7683^\circ\text{K}$, against $\rho - \rho_\lambda$, semilogarithmic plot. Equation of line: $(\rho\kappa_T)^{-1} = 1675.0 + 167.2 \log_{10}(\rho - \rho_\lambda)$.

to the fact that Lounasmaa had no data closer than 10^{-3} atm from the lambda point. Indeed, the present data would look much different if there were no points closer than 10^{-3} atm.

Our results are reported as $\rho\kappa_T = (\partial\rho/\partial P)_T$, rather than κ_T , since we have measured density changes, but not the absolute density. κ_T can be calculated from our data by dividing by 0.1797 g/cm^3 , the density at (T_λ, P_λ) obtained from Grilly and Mills' measurement⁴ at the upper lambda point and our measurement¹ of $(d\rho/dT)_\lambda$.

DISCUSSION

In order to correlate the compressibility data with the pressure-coefficient measurements, we make the assumptions that, over the small pressure and temperature range of these measurements, the lambda line is straight in the (P, T, ρ) space [$(dP/dT)_\lambda$ and $(d\rho/dT)_\lambda$ constant] and the isochores are congruent curves in the (P, T) plane whose slope is given [see (4) and (5)] by an equation of the form

$$\beta_V = A + B \ln|T - T_\lambda(\rho)|, \quad (10)$$

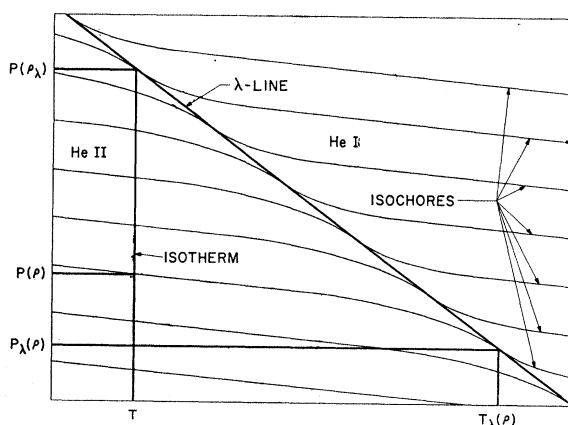


FIG. 8. Section of the P - T diagram of He⁴ (schematic), showing the λ line, several isochores, and an isotherm.

with A and B constant. A portion of the (P, T) plane, showing the lambda line and several isochores, is shown in Fig. 8 to illustrate our notation. When compressibilities are being measured, the sample point $[P(\rho), T]$ moves along the vertical line $T = \text{constant}$, passing from one isochore to another. The point $[P_\lambda(\rho), T_\lambda(\rho)]$ moves along the lambda line while $P(\rho_\lambda)$ and T remain constant, $[\rho_\lambda, P(\rho_\lambda)]$ being the point at which the isotherm $T = \text{constant}$ crosses the lambda line.

Now, it can be shown by the methods developed by Buckingham and Fairbank¹⁰ that

$$(\rho\kappa_T)^{-1} \equiv (\partial P/\partial \rho)_T = [(dP/dT)_\lambda - \beta_V]/(d\rho/dT)_\lambda. \quad (11)$$

Combining (10) and (11), and utilizing the fact that, since $(d\rho/dT)_\lambda$ is constant,

$$\rho_\lambda - \rho = (d\rho/dT)_\lambda [T - T_\lambda(\rho)], \quad (12)$$

we find

$$(\rho\kappa_T)^{-1} = C + D \ln |\rho - \rho_\lambda|, \quad (13)$$

where

$$C = [(dP/dT)_\lambda + B \ln |(d\rho/dT)_\lambda| - A]/(d\rho/dT)_\lambda, \quad (14)$$

$$D = -B/(d\rho/dT)_\lambda. \quad (15)$$

By integration of (13) at constant temperature, we find

$$P(\rho) - P(\rho_\lambda) = (\rho - \rho_\lambda)[C - D + D \ln |\rho - \rho_\lambda|]. \quad (16)$$

From Eqs. (1) and (2) in Ref. 1 we can calculate, for 5 mdeg above the upper lambda point,

$$(dP/dT)_\lambda = -56.02 \text{ atm}/^\circ\text{K}, \quad (17)$$

$$(d\rho/dT)_\lambda = -44.85 \times 10^{-3} \text{ g cm}^{-3}/^\circ\text{K}. \quad (18)$$

Substituting (17), (18), and the constants from (4) and (5) into (14) and (15), we find

$$C = 1038.2 \text{ atm cm}^3/\text{g} \quad (\text{He II}) \quad (19)$$

$$= 1675.0 \text{ atm cm}^3/\text{g}, \quad (\text{He I}) \quad (20)$$

$$D = 34.28 \text{ atm cm}^3/\text{g} \quad (\text{He II}) \quad (21)$$

$$= 72.62 \text{ atm cm}^3/\text{g} \quad (\text{He I}) \quad (22)$$

and, therefore,

$$(\rho\kappa_T)^{-1} = 1038.2 + 78.9 \log_{10}(\rho_\lambda - \rho) \text{ atm cm}^3/\text{g} \quad (\text{He II}) \quad (23)$$

$$= 1675.0 + 167.2 \log_{10}(\rho - \rho_\lambda) \text{ atm cm}^3/\text{g} \quad (\text{He I}), \quad (24)$$

$$P(\rho) - P(\rho_\lambda) = (\rho - \rho_\lambda)[1004.0 + 78.9 \log_{10}(\rho_\lambda - \rho)] \text{ atm} \quad (\text{He II}) \quad (25)$$

$$= (\rho - \rho_\lambda)[1602.4 + 167.2 \log_{10}(\rho - \rho_\lambda)] \text{ atm} \quad (\text{He I}). \quad (26)$$

In the He I region ($T > T_\lambda$), these equations fit the compressibility data fairly well, as indicated by the

¹⁰ M. V. Buckingham and W. M. Fairbank, in *Progress in Low-Temperature Physics*, edited by J. C. Gorter (North-Holland Publishing Company, Amsterdam, 1961), Vol. 3, p. 80.

solid lines in Figs. 5 and 7. In the He II region, the slope of Eq. (23) is correct, but the constant term is too large. In Figs. 5 and 6, Eq. (23) is represented by a dashed line.

A reason for this discrepancy is difficult to find. If $(dP/dT)_\lambda$ were not constant, or if an incorrect value were used in (14), it would affect the calculated compressibility in both He I and He II. It is hard to believe that the constants in Eq. (10) change appreciably in 0.2 mdeg, the total range of $T - T_\lambda(\rho)$ in the compressibility measurements, particularly when our earlier β_V data,¹ taken at a $T_\lambda(\rho)$ 5 mdeg lower, fit the same line as the present data.

Since β_V is the slope of an isochore, it cannot become larger in magnitude than $(dP/dT)_\lambda$, the slope of the lambda line, at the point where the isochore crosses the lambda line (see Fig. 8). Hence, β_V must deviate from the logarithmic relations (4) and (5) at some point very close to the lambda line. No restriction of this kind applies to κ_T . In fact, Buckingham and Fairbank¹⁰ have shown that κ_T must become infinite at the lambda line if, as seems probable,¹¹ the constant-pressure heat capacity becomes infinite there. The difficulty is rather that, if Eqs. (6) and (7) were correct, κ_T would become infinite before the lambda line was reached.

This should serve as a warning to anyone who tries to extrapolate his measurements to the lambda line. It is apparent that, at a few microdegrees from the lambda point, the limiting behavior of β_V has not yet become established, and this is likely to be true for other properties as well. For example, Rudnick and Shapiro,¹² who extrapolated their sound-velocity measurements (none of them closer to T_λ than 10^{-5} °K in He II and 10^{-4} °K in He I) to T_λ , suggested that there might be a discontinuity in the sound velocity at the lambda line, a possibility which is incompatible with a lambda-type transition. In view of the behavior of β_V , we doubt that the extrapolation functions used by Rudnick and Shapiro can be relied on to be valid for small values of $|T - T_\lambda|$.¹³

There seems little hope of improving the pressure-coefficient measurements substantially, but it would be well worthwhile to improve the precision of the compressibility measurements, to extend them somewhat closer to the lambda point, and to add one or two more decades away from the lambda point, in order to better establish the validity of (13), to evaluate the constants more accurately, and to investigate the discrepancy between the β_V and κ_T measurements in He II.

¹¹ W. M. Fairbank, M. V. Buckingham, and C. F. Kellers, in *Low-Temperature Physics and Chemistry*, edited by J. R. Dillinger (University of Wisconsin Press, Madison, Wisconsin, 1958), p. 50.

¹² I. Rudnick and K. A. Shapiro, *Phys. Rev. Letters* **15**, 386 (1965).

¹³ *Footnote added in proof.* Barmatz and Rudnick [Proceedings of the 10th International Conference on Low Temperature Physics, Moscow, U.S.S.R. (to be published)] have recently presented sound-velocity measurements to within 3.6 μdeg of the lambda point. When these new data are extrapolated to the lambda point, there is no discontinuity.